ChemComm

COMMUNICATION

View Article Online
View Journal | View Issue

Cite this: *Chem. Commun.*, 2024, **60**, 11774

Received 24th July 2024,
Accepted 19th September 2024

DOI: 10.1039/d4cc03721a

rsc.li/chemcomm

Synthesis of body temperature-triggerable dynamic liquid crystal elastomers using Diels–Alder crosslinkers†

Jérémy Baribeault St-Germain and Yue Zhao *

Novel liquid crystal elastomers (LCEs) with solely Diels–Alder dynamic covalent bonds (DADCBs) as crosslinks and body temperature sensitivity have been developed. The appealing attributes of the material, such as recyclability, reprogrammability and reconfigurability, have led to soft actuators capable of reversible deformation stimulated by shifting between ambient and body temperature, highlighting the potential for innovative applications in the biomedical field.

The thiol–acrylate Michael addition polymerization has become the most popular method for preparing soft liquid crystal elastomer (LCE) actuators.[1] With its modular "click" nature, it allows high yielding and efficient reactions to occur between monomers. Particularly useful for LCE actuators, the method has a great ease of adding comonomers in the precursor mixture for a desired effect or function. For instance, to impart an LCE actuator with photosensitivity, an azobenzene-containing comonomer can be introduced in the precursor mixture for reversible photoisomerization of the chromophore when exposed to light, leading to photocontrolled actuation.[2] Nevertheless, the use of the comonomer approach to prepare LCE actuators with dynamic covalent bonds (DCBs) for crosslinking has been very little explored despite the growing interest on DCB-based LCEs.[3–9] To this regard, most notably Cai and coworkers introduced dynamic disulfide bonds in the LCE by controlling the thiol–acrylate reactions of common monomers and used the disulfide metathesis reaction to convert polydomain to monodomain LCE required for actuation.[10]

The purpose of the present work is to design and synthesize dynamic LCEs *via* the thiol–acrylate Michael addition method, and to investigate the actuation of novel LCEs that have two specific properties: (1) the LCEs have an order-to-disorder (nematic-to-isotropic) phase transition occurring at a temperature (T_{NI}) between 25 °C and 37 °C, leading to body temperature-triggerable LCE actuators that are promising for biomedical applications.[11,12] (2) The crosslinking of the LCEs is solely made of Diels–Alder (DA) DCBs, making the actuators reprogrammable, reconfigurable and recyclable.

Our design is to use a non-mesogenic diacrylate comonomer bearing a furan group for both tuning the T_{NI} and forming the DA crosslinks by reacting with bismaleimide molecules present in the LCE. On one hand, the furan-maleimide coupling is a common approach to obtain highly reversible DA crosslinks in a polymer network.[13] On the other hand, the dilution of the mesogenic components in an LCE by adding a non-mesogenic comonomer has the effect of reducing the T_{NI}.[14] Our hypothesis is that the DA adduct at an appropriate content in such an LCE could act as both the reversible crosslinks ensuring the actuating properties and the non-mesogenic diluent bringing the T_{NI} into the desired temperature range. As shown below, the outcome of this study has validated this design principle.

Fig. 1a shows the chemical structures of all the monomers used (synthesis and characterization details in ESI†). In addition to the commercially available RM257 (LC mesogen) and EDDET (chain extender), two furan-containing comonomers, RMF (2-(furan-2-ylmethyl)-1,4-phenylenebis(4-(3-(acryloyloxy)propoxy)-benzoate)) and BAMF (furan-2,5-diylbis(methylene)diacrylate), were synthesized, and BM is the bismaleimide used as crosslinker. While RMF has a bulky and similar structure to RM257 and has a lateral furan group with respect to chain backbone, BAMF has a smaller and more rigid structure, and its furan group is part of the chain backbone in the resulting LCE. By using both RMF and BAMF (separately), possible effect of comonomer structure on T_{NI}, DA bond formation and actuation behaviours could be unveiled. However, with our precursor mixture design without the traditional crosslinker (PETMP: pentaerythritol tetrakis(3-mercaptopropionate)) used in most, if not all, LCEs synthesized through the thiol–acrylate Michael

Département de chimie, Université de Sherbrooke, 2500 Bd de l'Université, Sherbrooke, Québec, Canada. E-mail: yue.zhao@usherbrooke.ca

† Electronic supplementary information (ESI) available: Experimental details, ^{1}H and ^{13}C NMR and HRMS spectra for the compounds, data of kinetic study, table of thermal phase transitions data, DSC scan and POM images of the RMF comonomer, POM images of monodomain R25DA and B15DA, recyclability test, ATR-FTIR spectra showing polymerization and reversible DA crosslinks, movies showing the actuation of R25DA and B15DA. See DOI: **https://doi.org/10.1039/d4cc03721a**

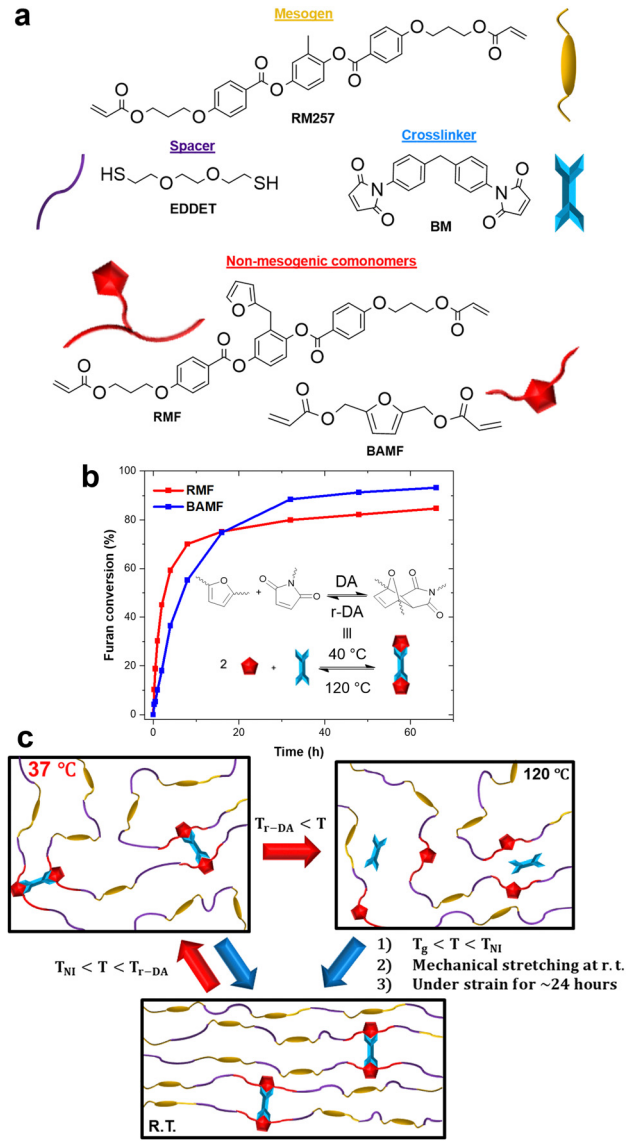

Fig. 1 (a) Chemical structures and acronyms of the monomers used to synthesize dynamic LCEs. (b) Plots of furan conversion *vs.* reaction time for the non-mesogenic comonomers reacting with bismaleimide to form the DA adduct. (c) Schematic illustration of the preparation process of the DADCB LCE actuator capable of reversible deformation upon heating and cooling across the T_{NI} (T = LCE temperature) (see text for details).

addition polymerization, two potential issues arose. Firstly, if the network formed contains an insufficient number of DA crosslinks, it lacks structural integrity and mechanical strength for deformation, but a large amount of bismaleimide in the mixture may undergo phase separation before completion of DA crosslinking. Secondly, by mixing the bismaleimide with the monomers, it would lead to undesirable side reactions during the polymerization between the maleimide and thiol groups due to the high reactivity of the vinyl group in the maleimide ring,[1] which interferes or even prevents the desired formation of DA crosslinks between the furan–maleimide couple.

Our approach to address the two problems is to use furan-protected maleimide, known in structure-tailored polymer synthesis.[15] More specifically, DA adduct comonomers were first synthesized through reaction between RMF and BM or BAMF and BM as latent reversible crosslinks and then used in the thiol-Michael addition polymerization. This would fend off any side reactions on the maleimide in the cycloadduct structure. It also directly leads to an DADCB-crosslinked LCE ready for mechanical deformation. Afterwards, the DA crosslinking density can be easily adjusted by heating the LCE to an elevated temperature for retro DA reaction ($T_{r\text{-}DA}$), and partially DA-crosslinked LCEs can be mechanically stretched in the LC phase to induce the alignment of mesogens followed by formation of more DA crosslinks at room temperature to self-lock the monodomain LCE with reversible actuation.[16]

The synthesis of the monodomain LCEs starts with the protection of the maleimide functions by mixing the BM (1 eq.) with either one of the furan comonomers (2 eq.) and a small quantity of hydroquinone inhibitor (0.5 wt% to bulk). The mixture is then left at 40 °C and monitored by ^{1}H NMR until the reaction completion (Fig. S9 and S10, ESI†). The integration of the peaks of protons in the furan group was used to determine the conversion of furan as function of time (Fig. 1b). The result shows that RMF reacts with BM faster than BAMF does within the first 10 h, but the ceiling conversion ratio appears to be higher with BAMF. Then, the formed DA adduct is purified by column chromatography and mixed with RM257, EDDET and trace amounts of dipropylamine (DPA, catalyst) in the appropriate quantity to obtain the desired composition. Subsequently, the mixture is poured into a mold and left at room temperature overnight for a one-pot thiol–acrylate Michael addition polymerization. The polymerization is followed by recording ATR-FTIR spectra, where the band at 810 cm^{-1} corresponding to the twisting of the C=C bond in the acrylate group disappears when the polymerization is done (Fig. S15, ESI†).[17] After drying *in vacuo* at 40 °C for 24 hours, the DA-crosslinked LCE is obtained. The schematic in Fig. 1c illustrates how the as-prepared polydomain LCE is typically processed to monodomain LCE actuator. First, it is heated to $T_{r\text{-}DA}$ (~120 °C) for 1 to 3 minutes, depending on the sample's dimension, to break a fraction of the DA crosslinks. Next, it is cooled to room temperature, between T_{NI} and T_g (glass transition temperature) in the nematic phase, and mechanically stretched to about 100% strain (or deformed to a desired shape) inducing the alignment of mesogens in the strain direction. Finally, the deformed shape is retained at room temperature for 24 h to let the DA crosslinks reform and lock the programmed monodomain shape in memory to obtain an actuator.[16]

Multiple compositions of polydomain LCEs were synthesized containing BAMF or RMF and their thermal phase transitions were measured using DSC (Table S1, ESI†). The substitution of RM257 in the network by one of the comonomers led to a decrease of the T_{NI} and an increase of the enthalpy of the retro-DA reaction (Fig. 2a). The effect of the non-mesogenic comonomer moieties on the T_{NI} of the resulting LCE can be seen from the plot of T_{NI} *vs.* mol% of LC mesogenic groups (Fig. 2b). With the RMF comonomer, T_{NI} between 25 °C and 37 °C was achievable for compositions with 20 and 25 mol% of the acrylate groups belonging to the non-mesogenic comonomer (the samples are

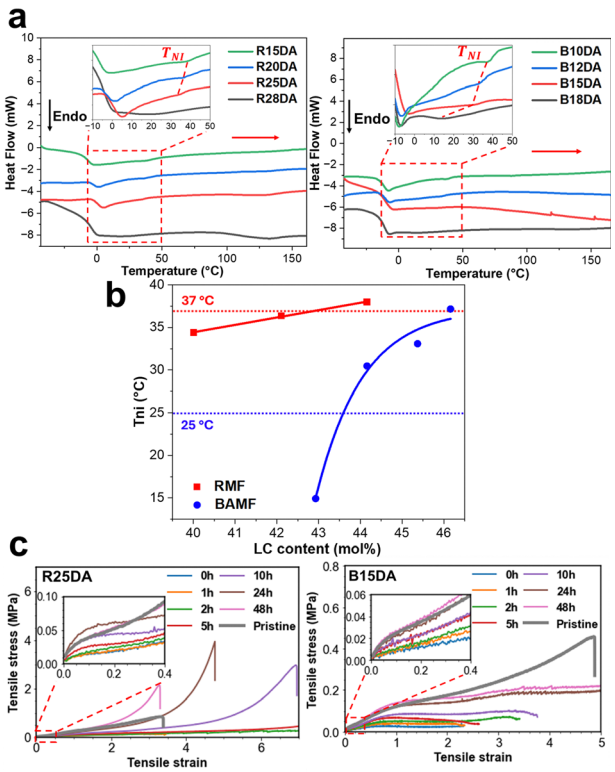

Fig. 2 Characterization of the polydomain LCEs synthesized with furan-containing, non-mesogenic comonomer of RMF or BAMF (the sample acronyms start with R or B for the two comonomers, followed by a number that is the mol% of acrylate groups in the comonomer). (a) DSC heating scans with an inset showing a magnified region containing the endothermic nematic-to-isotropic phase transition (T_{NI}) of the LCEs. (b) Plots of T_{NI} *vs.* the liquid crystal molar content in the LCEs containing either RMF or BAMF. The target T_{NI} values are located between the two dotted lines in the graph. (c) Tensile tests of two polydomain LCEs (R25DA and B15DA) conducted after different waiting times at room temperature following cooling from 120 °C, with the inset showing the magnified starting region at small strains.

denoted as R20DA and R25DA, respectively). With the BAMF, the 12 and 15 mol% compositions led to the desired T_{NI} of the LCE (B12DA and B15DA). Considering that RMF has a similar structure to RM257, and the BAMF's smaller and more rigid structure is less compatible with RM257, it is no surprise to observe BAMF acting as a more efficient non-mesogenic diluent leading to a bigger impact on the T_{NI}.[14] Following the DSC analysis, the LCEs of R25DA and B15DA, fulfilling the criterion of body temperature sensitivity, were selected for further investigations. Before reporting the actuation properties, tensile tests were performed on polydomain samples of R25DA and B15DA after different waiting times at room temperature following cooling from 120 °C (20 min retro-DA reaction). The results in Fig. 2c show that with increasing the waiting time the sample displays an increased Young's modulus (the slope of the curve at small strains) and a decreased strain at break, which is characteristic of a sample with increasing crosslinking density, and which confirms the slow formation of DA bonds at room temperature. After 24 h waiting, the mechanical properties are greatly recovered with respect to the pristine sample (before dissociating DA bonds at 120 °C). The revisable crosslinking and de-crosslinking in the LCEs through DA and retro-DA reaction, respectively, was further confirmed by ATR-FTIR spectral changes upon repeated heating/cooling cycles of the LCEs (Fig. S16, ESI†).[13]

The actuation performance of the dynamic LCEs was investigated with R25DA and B15DA. By heating and cooling their monodomain strips between body (37 °C) and room temperature (about 25 °C), which crosses their respective T_{NI}, the film shrinks in length on heating and extends on cooling, while measuring the length in the isotropic (37 °C) and nematic phase (r.t.) allows the reversible actuation degrees (RAD, defined in Fig. 3a) to be determined. The reversible deformation of the monodomain strips of both R25DA and B15DA was observed over 10 consecutive cycles of heating and cooling, showing stable actuation (Fig. 3a and Movie S1, ESI†). Moreover, the RAD values of 30% and 34% were obtained for R25DA and B15DA, respectively, which is highly efficient for low temperature actuation. As confirmed by 2D wide angle X-ray scattering (2D-WAXS) (Fig. 3b) measurements and polarized optical microscopy (POM) (Fig. S17, ESI†), the reversible actuation originates from the order-to-disorder transition of the aligned mesogens in the LCEs. At room temperature, the mesogens are macroscopically aligned along the long axis of the strip (the stretching direction in the actuator preparation process),

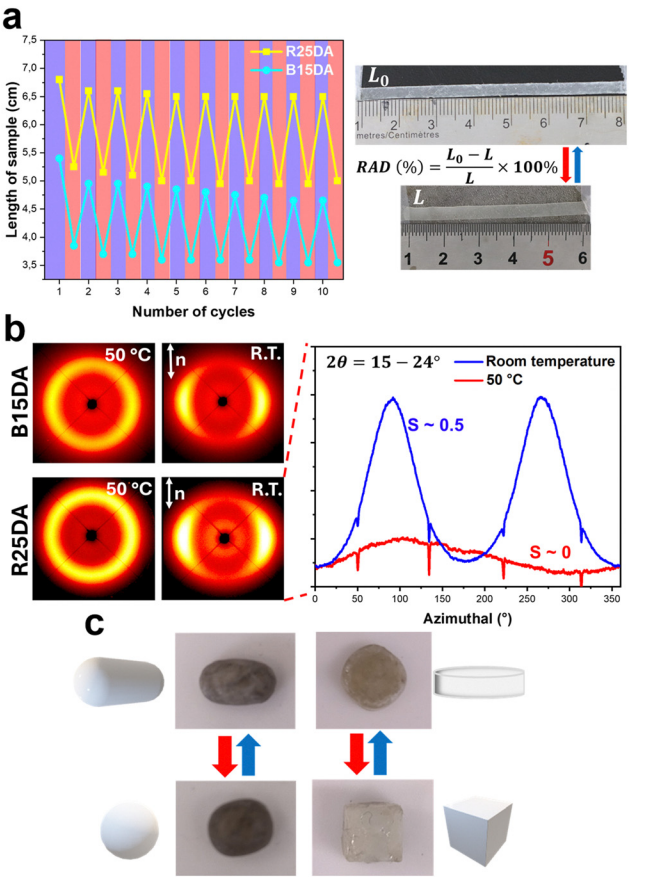

Fig. 3 Actuation of monodomain B15DA and R25DA. (a) Change of length over repeated cycles of heating to 37 °C and cooling to room temperature, with photographs showing the reversible contraction and extension of an LCE strip. (b) 2D-WAXS patterns and azimuthal profiles for the R25DA at room temperature and in the isotropic state. (c) 3D bulk reversible actuation of R25DA.

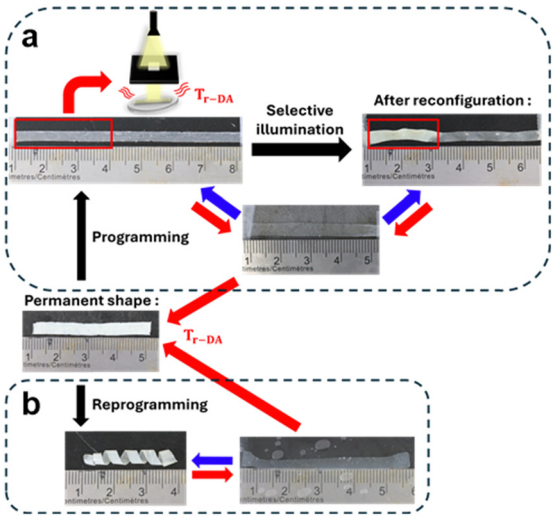

Fig. 4 Photographs demonstrating (a) the reconfigurability and (b) reprogrammability of the dynamic LCE actuator on B15DA (see text for details).

giving rise to diffraction arcs on equator. The azimuthal profile at the corresponding diffraction angles reflects the alignment degree characterized by the order parameter defined as $S = (3\cos^2\phi - 1)/2$, where ϕ is the angle between the long axes of the actuator strip and LC mesogen. For both the monodomain R25DA and B15DA, an order parameter of $S \sim 0.5$ was obtained at room temperature ($S = 1$ for perfect alignment and $S = 0$ for absence of alignment). When heated to the isotropic state, the mesogens become disordered. In addition to the 2D LCE actuator in the form of thin film, 3D bulk actuator can also be obtained by using the aforementioned, DADCB-enabled actuator fabrication procedure. To demonstrate this, a cube and a sphere of R25DA were first prepared by moulding (Fig. 3c), after heating to $T_{r\text{-}DA}$ for 3 min and then cooling to room temperature, the cube was compressed into a "pie" geometry and the sphere was stretched to form an ellipsoid; after holding the deformed state for 24 h to allow DA crosslinks to form and lock the deformed state, 3D bulk actuators displaying reversible geometry change were fabricated (Fig. 3c and Movies S2, S3, ESI†).

The different attributes of these LCEs were then explored (Fig. 4). On the one hand, we tested the actuator reconfigurability using B15DA. A monodomain LCE strip was first programmed, and it exhibits reversible contraction and extension upon heating (37 °C) and cooling (r.t.) respectively. The same actuator was then optically reconfigured to exhibit a changed actuation. To this end, a region of the strip was selectively heated to $T_{r\text{-}DA}$ by flashlight illumination (FlashTorch 100, Wicked Lasers) generating a photothermal effect (Fig. S18, ESI†), while the rest of the strip was masked; after turning off the light, the cooled illuminated region became polydomain and non-actuating. Under the same heating and cooling stimulation, the LCE strip contracts and extends differently (shorter at room temperature). On the other hand, the dynamic LCE afford the actuator reprogrammability thanks to its abilities to be recyclable (Fig. S19, ESI†), meaning that the LCE can be used as starting material to fabricate a different actuator. As also shown in Fig. 4, where the whole B15DA sample was heated at $T_{r\text{-}DA}$, then reprogrammed into an helicoidal shape. In this case, instead of extending upon cooling under its T_{NI}, it rolls into an helicoidal shape (Movie S4, ESI†), which is completely reversible. These experiments demonstrate the many possibilities for different macroscopic deformations, while using the same sample.

In conclusion, we have developed novel LCE actuators containing only DADCBs as crosslinks, and whose reversible deformation can be triggered by temperature change between room and body temperature (25 to 37 °C). Such dynamic LCEs were synthesized using the thiol–acrylate Michael addition polymerization while replacing in the precursor mixture the traditional PETMP crosslinker with a diacrylate comonomer containing a furan-maleimide DA adduct, which serves as both the dynamic DA crosslinker and the non-mesogenic diluent for the T_{NI} tuning. We showed that the easy control of the DA crosslinking density, due to the slow DA bond formation at room temperature after retro-DA reaction, facilitates the fabrication of LCE actuators as well as their reprogramming and reconfiguration. Particularly worth mentioning is the body temperature sensitive 2D and 3D bulk LCE actuator for potential applications in actuating biomedical devices.

Data availability

All data can be found in the main article or the ESI.†

Conflicts of interest

There are no conflicts to declare.

Notes and references

1 D. P. Nair, M. Podgórski, S. Chatani, T. Gong, W. Xi, C. R. Fenoli and C. N. Bowman, *Chem. Mater.*, 2014, **26**, 724–744.
2 E. Cho, K. Luu and S. Park, *Macromolecules*, 2021, **54**, 5397–5409.
3 M. O. Saed, A. Gablier and E. M. Terentjev, *Chem. Rev.*, 2022, **122**, 4927–4945.
4 T. J. White and D. J. Broer, *Nat. Mater.*, 2015, **14**, 1087–1098.
5 X. Lu, S. Guo, X. Tong, H. Xia and Y. Zhao, *Adv. Mater.*, 2017, **29**, 1606467.
6 Y. Wu, Y. Yang, X. Qian, Q. Chen, Y. Wei and Y. Ji, *Angew. Chem., Int. Ed.*, 2020, **59**, 4778–4784.
7 T. Ube, K. Kawasaki and T. Ikeda, *Adv. Mater.*, 2016, **28**, 8212–8217.
8 M. K. McBride, M. Hendrikx, D. Liu, B. T. Worrell, D. J. Broer and C. N. Bowman, *Adv. Mater.*, 2017, **29**, 1606509.
9 X. Lu, C. P. Ambulo, S. Wang, L. K. Rivera-Tarazona, H. Kim, K. Searles and T. H. Ware, *Angew. Chem., Int. Ed.*, 2021, **60**, 5536–5543.
10 Z. Wang, H. Tian, Q. He and S. Cai, *ACS Appl. Mater. Interfaces*, 2017, **9**, 33119–33128.
11 H. Kim, J. Li, Y. S. Y. Hsieh, M. Cho, S. Ahn and C. Li, *Small*, 2022, **18**, 2203772.
12 M. Li, A. Pal, A. Aghakhani, A. Pena-Francesch and M. Sitti, *Nat. Rev. Mater.*, 2021, **7**, 235–249.
13 T. T. Truong, H. T. Nguyen, M. N. Phan and L. T. Nguyen, *J. Polym. Sci., Part A: Polym. Chem.*, 2018, **56**, 1806–1814.
14 M. Barnes, S. Cetinkaya, A. Ajnsztajn and R. Verduzco, *Soft Matter*, 2022, **18**, 5074–5081.
15 Y. Ji, L. Zhang, X. Gu, W. Zhang, N. Zhou, Z. Zhang and X. Zhu, *Angew. Chem., Int. Ed.*, 2017, **56**, 2328–2333.
16 Z. Jiang, Y. Xiao, L. Yin, L. Han and Y. Zhao, *Angew. Chem., Int. Ed.*, 2020, **59**, 4925–4931.
17 M. O. Saed, A. H. Torbati, D. P. Nair and C. M. Yakacki, *J. Visualized Exp.*, 2016, 53546.